A&A 548, A26 (2012)
DOI: 10.1051/0004-6361/201219984

Astronomy & Astrophysics

CFBDSIR2149-0403: a 4–7 Jupiter-mass free-floating planet in the young moving group AB Doradus?⋆

P. Delorme[1], J. Gagné[2], L. Malo[2], C. Reylé[3], E. Artigau[2], L. Albert[2], T. Forveille[1], X. Delfosse[1], F. Allard[4], and D. Homeier[4]

[1] UJF-Grenoble 1/CNRS-INSU, Institut de Planétologie et d'Astrophysique de Grenoble (IPAG) UMR 5274, 38041 Grenoble, France
e-mail: Philippe.Delorme@obs.ujf-grenoble.fr
[2] Département de physique and Observatoire du Mont Mégantic, Université de Montréal, CP 6128, Succursale Centre-Ville, QC H3C 3J7 Montréal, Canada
[3] Université de Franche Comté, Institut UTINAM CNRS 6213, Observatoire des Sciences de l'Univers THETA de Franche-Comté, Observatoire de Besançon, BP 1615, 25010 Besançon Cedex, France
[4] CRAL, UMR 5574 CNRS, École Normale Supérieure, 69364 Lyon Cedex 07, France

Received 11 July 2012 / Accepted 25 September 2012

ABSTRACT

Using the CFBDSIR wide field survey for brown dwarfs, we identified CFBDSIRJ214947.2-040308.9, a late T dwarf with an atypically red $J - K_S$ colour. We obtained an X-Shooter spectra, with signal detectable from 0.8 μm to 2.3 μm, which confirmed a T7 spectral type with an enhanced K_s-band flux indicative of a potentially low-gravity, young object. The comparison of our near infrared spectrum with atmosphere models for solar metallicity shows that CFBDSIRJ214947.2-040308.9 is probably a 650−750 K, $\log g$ = 3.75−4.0 substellar object. Using evolution models, this translates into a planetary mass object with an age in the 20−200 Myr range. An independent Bayesian analysis from proper motion measurements results in a 87% probability that this free-floating planet is a member of the 50−120 Myr-old AB Doradus moving group, which strengthens the spectroscopic diagnosis of youth. By combining our atmospheric characterisation with the age and metallicity constraints arising from the probable membership to the AB Doradus moving group, we find that CFBDSIRJ214947.2-040308.9 is probably a 4−7 Jupiter mass, free-floating planet with an effective temperature of ∼700 K and a $\log g$ of ∼4.0, typical of the late T-type exoplanets that are targeted by direct imaging. We stress that this object could be used as a benchmark for understanding the physics of the similar T-type exoplanets that will be discovered by the upcoming high-contrast imagers.

Key words. stars: atmospheres – planets and satellites: atmospheres – surveys – methods: observational – techniques: spectroscopic – brown dwarfs

1. Introduction

The International Astronomical Union definition[1] that the planetary mass range is below deuterium-burning mass (13 $M_{\rm Jup}$; Boss et al. 2003), while brown dwarfs and stars populate the mass range above is challenged by a string of recent discoveries, notably from possible isolated planetary mass objects (hereafter IPMOs, or equivalently free-floating planets in clusters, see for instance Zapatero Osorio et al. 2002; Burgess et al. 2009; Marsh et al. 2010; Haisch et al. 2010; Peña Ramírez et al. 2011, 2012; Scholz et al. 2012), which are more likely formed like stars but reside in the planetary mass range. There are also many cases of field brown dwarfs whose lower mass limit is well within the official planetary mass range (see for instance Knapp et al. 2004; Burgasser et al. 2006; Cruz et al. 2009; Lucas et al. 2010; Burningham et al. 2011b; Liu et al. 2011; Luhman et al. 2011; Cushing et al. 2011; Albert et al. 2011). However, in all these cases there are significant uncertainties on the actual masses of these possibly free-floating planets, mostly because of the age/mass/luminosity degeneracy that affects the determination of the physical parameters of substellar objects. This degeneracy can be lifted when the age of the source can be constrained independently, usually through cluster or association membership. There is, however, no isolated object that combines such an undisputed age constraint with spectroscopic low-gravity signatures that would be compatible with a planetary mass.

There is nonetheless strong evidence that IPMOs do exist, at least since the discovery of 2M1207B by Chauvin et al. (2004) has established the existence of a ∼5 $M_{\rm Jup}$ companion around a ∼25 $M_{\rm Jup}$ object that would be almost impossible to form through planetary formation mechanisms. This means stellar formation processes, such as cloud fragmentation (see for instance Bate 2009) or disk fragmentation (see for instance Stamatellos et al. 2011), can form planetary mass objects. Peña Ramírez et al. (2012) has recently identified a population of IPMOs in the σ-Orionis cluster, and hinted that they could be about as numerous as deuterium-burning brown dwarfs. This would indicate that there is a significant population of overlooked IPMOs in the solar vicinity, both in the field and in young moving groups and clusters. Another source of IPMOs could be ejected planets (e.g. Veras & Raymond 2012; Moeckel & Veras 2012), since massive planets such as HR8799bcde (Marois et al. 2008, 2010), if ejected from their host star, would look like regular field T dwarfs after a few hundred Myr. Another strong proof

⋆ Based on observations obtained with SOFI on the NTT at ESO-La Silla (run 086.C-0655(A)). Based on observations obtained with X-Shooter on VLT-UT2 at ESO-Paranal (run 087.C-0562(A)). Based on observations obtained with WIRCAM at CFHT (programmes 09AF21, 10BF26, and 11BD86).

[1] http://www.dtm.ciw.edu/boss/definition.html

that IPMOs exist is the detection of a few free-floating planets by gravitational lensing by Sumi et al. (2011) and Strigari et al. (2012), though these objects – or at least a fraction of them – could also be regular planets orbiting at a large enough separation from their host star that the latter is not detectable in the lensing event.

The detection of IPMOs can therefore provide constraints on ejection scenarii and on the low-mass end of the stellar mass function, though these constraints will not be independent since it is observationally challenging to imagine a way to distinguish between a 5 $M_{\rm Jup}$ ejected planet and a brown dwarf of the same mass. However, the spectral energy distribution (SED) of these isolated objects will provide useful information on the substellar evolution and substellar atmosphere models, especially if their age is known, and regardless of their formation mechanisms. These constraints are especially valuable because the SED of an IPMO is expected to be identical to the SED of planets with similar masses orbiting at large separations – hence with negligible irradiation – from their host stars. In this light, such free-floating planets could serve as benchmarks for the design and operation of the direct imaging surveys for exoplanets, notably with the upcoming new generations planets finder instruments, such as SPHERE (Beuzit et al. 2008), GPI (Graham et al. 2007), or HiCIAOH (Hodapp et al. 2008). Young IPMOs of a few Jupiter masses would be interesting analogues of the exoplanets these instruments will be able to detect. Since they are not affected by the glare of a host star, it is comparatively easy to obtain relatively high signal-to-noise ratio (S/N), moderate-resolution spectroscopic information so that they can serve as prototypes for understanding the physics of massive exoplanets' atmospheres.

We present in Sect. 2 the detection of a low-gravity T dwarf, CFBDSIRJ214947.2-040308.9, hereafter CFBDSIR2149, which is probably a 4−7 $M_{\rm Jup}$ free-floating planet. In Sect. 3, we describe our spectroscopic data reduction and present the full near-infrared (NIR) spectrum of this object, highlighting its low-gravity features. In Sect. 4 we discuss its likely membership to the young moving group AB Doradus (hereafter ABDMG). In Sect. 5 we analyse its spectrum in the light of the age and metallicity constraints that would be brought by its probable ABDMG membership, and derive its fundamental physical parameters. Finally we discuss some of the implications of this discovery.

2. Photometry of CFBDSIR2149

2.1. Discovery and identification as a late T dwarf with K_s-band excess

The Canada-France Brown Dwarf Survey InfraRed (CFBDSIR; Delorme et al. 2010) is an NIR coverage of the CFHTLS/CFBDS (see Delorme et al. 2008b) fields with available deep z' band images. It covers 335 square degrees with J-band WIRCam (Puget et al. 2004) images. Cool brown dwarfs candidates are identified from their very red $z' - J$ colour (see Fig. 2), and CFBDSIR2149 was identified as such by the standard CFBDSIR analysis pipeline (see Delorme et al. 2010). After analysing and cross-matching a stack of two 45 s-long WIRCam J-band exposure from the CFBDSIR acquired on August 13 and 14, 2009, with the corresponding CFBDS-RCS2 (Yee et al. 2007; Delorme et al. 2008b) 360 s z' exposure, we highlighted CFBDSIR2149 as a z' dropout with $z' - J > 3.8$.

This promising candidate was confirmed by NIR follow-up observations at the ESO-NTT telescope (run 086.C-0655(A)) on September 24, 2010 with an NTT-Sofi (Moorwood et al. 1998),

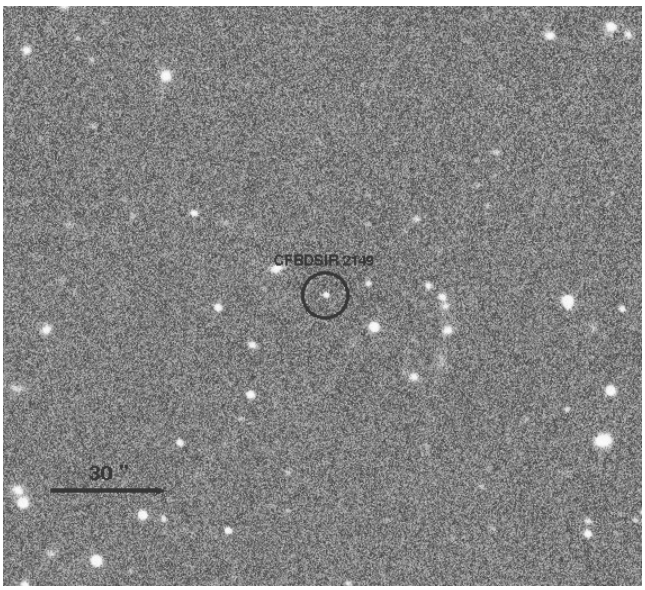

Fig. 1. Finding chart for CFBDSIR2149 (Js-band NTT Sofi image). East is left and north is up.

J-band detection (see Fig. 1) ensuring that this candidate was a very cool brown dwarf and not a transient source, such as an extragalactic supernovae or an asteroid that could have caused our initial J-band detection and accounted for the z'-band non-detection. The real-time analysis of the NTT J-band data prompted further observations of this cool brown dwarf in H and K_s, during the following night. The resulting very blue $J - H = -0.5$ confirmed it as a very late T dwarf, while the neutral to red $J - K_s \sim 0$ highlighted it as a peculiar K_s-band flux enhanced late T dwarf (see Fig. 2). Throughout this work, $YJHK/K_s$ magnitudes are given in the Vega system, while z' mags are in the AB system (Fukugita et al. 1996).

2.2. Near-infrared imaging: reduction and analysis

In addition to this SOFI photometric follow-up, we obtained higher S/N photometric data in Y, J, and K_s from CFHT Director Discretionary Time in December 2011, as well as CH_{4on} imaging acquired in September 2010. This WIRCam data, using the MKO photometric system, is deeper and offers a larger time base to derive the proper motion of CFBDSIR2149 using the WIRCam 2009 August detection images as a first epoch. Since WIRCam has a larger field of view than SOFI it also allows using more stars for an accurate photometric and astrometric calibration.

Both SOFI and WIRCam observations used a standard dithering pattern to allow the construction of a sky frame, and they were reduced and analysed using the same home-made pipeline. For the WIRCam observations, we used one (out of 4) $10' \times 10'$ chips, on which the target was centred. For each filter, flat fielding and bad pixel removal were carried out using ESO-*eclipse* software package (Devillard 2001). A sky frame, constructed by median-combining the dithered raw exposures, was subtracted from each exposure. The resulting reduced individual exposures were cross-matched using *Scamp* (Bertin 2006) and combined with *Swarp* (Bertin 2010), using the inverse of each image background noise as weight. This weighting particularly improved the S/N of the WIRCam images which were acquired with a rapidly evolving airmass, while the target was setting. The

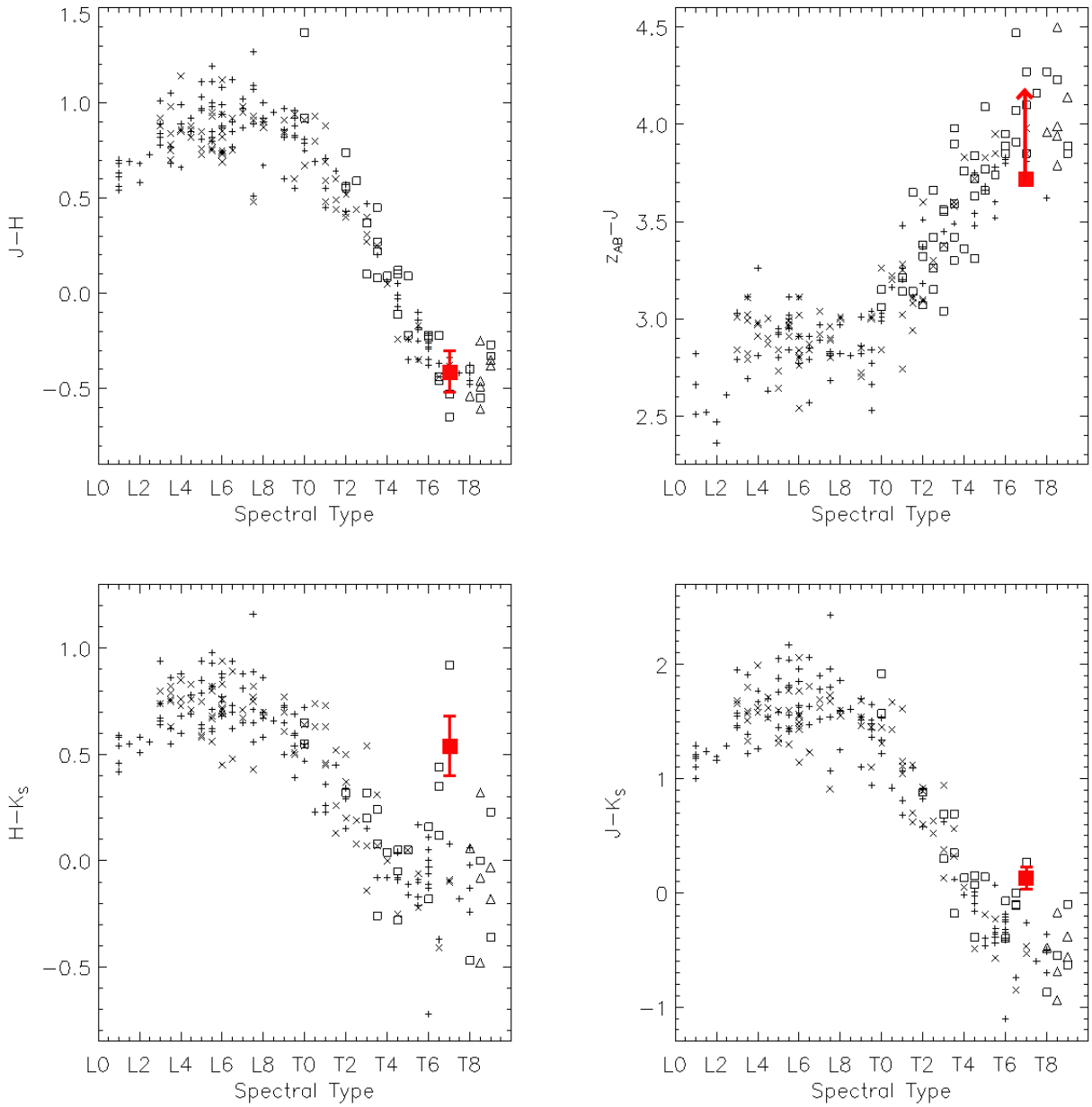

Fig. 2. Near-IR MKO colours of CFBDSIR2149 (red square) compared to known field T dwarfs. The arrows in $z' - J$ colours indicates this colour is a lower limit since we have no z'-band detection. Open squares are CFBDS T dwarfs Albert et al. (2011), the plus signs are 111 dwarfs from Knapp et al. (2004), crosses are 73 dwarfs from Chiu et al. (2006) while open triangles are late T dwarfs from Burningham et al. (2008, 2009, 2010), Delorme et al. (2010), and Lucas et al. (2010).

absolute astrometric and photometric calibrations in J, H, and K_s were carried out using the 2MASS point source catalogue (Cutri et al. 2003) as a reference, with three valid references on the SOFI field of view and 15 on the WIRCam chip field of view. For the photometric calibration of z', Y, and CH_{4on} data, we used the CFHT-provided zero points and absorption values.

We extracted the photometry and astrometry of CFBDSIR2149 and of the reference stars by point spread function (PSF) fitting using *Sextractor*, with a spatially variable PSF model built from each science image using *PSFex* (Bertin & Arnouts 1996; Bertin 2006; Bertin et al. 2012). The resulting photometry is shown in Table 1. The $H - CH_{4on}$ of 0.9, tracing the methane absorption bands around 1.6 μm is typical of a T7 ± 0.5 brown dwarf (calibration by Albert, priv. comm.), while the red $J - K_s$ and very red $H - K_s$ (see Fig. 2) indicate a weak collision induced absorption of H_2 (CIA), resulting in an enhanced K-band flux (see Knapp et al. 2004, for instance). The weak CIA would be caused by a lower than usual pressure in the photosphere, either due to low gravity, high metallicity, or a combination of both. We caution that such a colour diagnosis can be misleading, at least for objects in the L/T transition, where cloud coverage effects can blur the conclusions (see the unusual blue and red $J-K$ in the T2.5/T4 binary of Artigau et al. 2011). However the later spectral type of CFBDSIR2149 (T7) places it in a temperature range where models, and the associated colour diagnosis, are usually more reliable, mainly because most clouds have condensated at such low temperatures. This also makes the red $J - K$ association with low gravity/high metallicity more robust for late T dwarfs such as CFBDSIR2149 than it is for the red, also probably low-gravity, L dwarfs identified by Cruz et al. (2009), Allers et al. (2010), and Faherty et al. (2012).

Table 1. Photometry of CFBDSIR2149 with NTT and CFHT.

	z'_{ab}	Y	J	H	K_s	CH_{4on}
CFHT	>23.2 (360 s)	20.83 ± 0.09 (936 s)	19.48 ± 0.04 (540 s)	–	19.35 ± 0.09 (880 s)	20.7 ± 0.25 (900 s)
Date	05/07/2006	18,26/12/2011	18,26/12/2011	–	18,26/12/2011	29/09/2010
NTT	–	–	19.48 ± 0.04 (720 s)	19.89 ± 0.11 (600 s)	19.54 ± 0.14 (1200 s)	–
Date	–	–	23/09/2010	24/09/2010	24/09/2010	–

Notes. The corresponding exposure time is indicated in parentheses.

2.2.1. WISE data

We searched the WISE (Wright et al. 2010) all-sky release catalogue for a mid-infrared couterpart of CFBDSIR2149. There is no signal related to our target in W3 and W4 channels, but we found a very faint object at its exact position in W2 and slightly offset in W1. The catalogue-provided photometry for this couterpart gives W1 = 17.4 ± 0.47 and W2 = 15.99 ± 0.37. Though this mid-infrared S/N is extremely low, the resulting $H - W2 = 3.9 \pm 0.4$ colour is consistent with CFBDSIR2149 being a late T dwarf (see Fig. 1 of Mainzer et al. 2011).

3. Spectroscopy of CFBDSIR2149

3.1. Spectroscopic follow-up and reduction

Given the faintness ($J = 19.3$) of CFBDSIR2149, it was not observed in spectroscopy with Sofi at NTT and was therefore put in the queue of our 087.C-0562 ESO-VLT X-Shooter observations as a very high priority target. It was observed on September 5 and September 27, 2011 in two ESO observing blocks (hereafter OB), achieving a total exposure time on target of 5850 s, split into four A-B nods on slits of 2 × 732 s each. We used 0.9″ slits for both visible and NIR arms.

The spectra were reduced using the latest ESO X-Shooter pipeline (Modigliani et al. 2010), which produced a two-dimensional, curvature-corrected spectrum of the NIR arm of X-Shooter from 0.99 to 2.5 μm and of the visible arm, from 0.6 to 1.02 μm for each OB. No signal was retrieved for wavelengths shorter than ∼0.8 μm, but a low S/N spectrum of the optical farred was recovered between 0.8 and 1.0 μm. The trace was extracted using our own IDL procedures, using Gaussian boxes in the spatial dimension all along the spectral direction. The noise spectrum was obtained by measuring the dispersion along ten spectral pixels on a noise trace obtained by subtracting the science trace by itself shifted of one pixel. Since the shift is much smaller than the full spectral resolution (4.2 pixels in the NIR and 6.0 in the visible), this effectively removes the science spectrum, but keeps the information on the actual background and photon noise on the science trace.

The two resulting one-dimensional spectra of each OB were then divided by the spectrum of telluric standard stars observed just after or just before each OB and reduced and extracted using the same pipeline as the science OBs. The two spectra corrected from telluric absorption were then combined through a weighted average using the inverse variance as weight to construct the science spectrum. A noise-weighted average significantly improved the S/N since the quality of data obtained on September 5 was noticeably better than obtained on September 27. Because the resulting spectrum at $R \sim 5300$ has a low S/N and most of the late T physical parameters exploration is carried out using lower resolution spectra, we made a sliding noise-weighted average on 25, 100 and 200 pixels in the spectral dimension, producing three spectra, at a resolution of respectively $R = 900$, 225, and 113 in the NIR. The visible spectra was similarly binned on 400 pixels, with a corresponding resolution $R = 132$. The noise-weighted average in the spectral dimension makes use of the full resolution of X-Shooter to down-weight the narrow wavelength ranges affected by OH telluric emission lines, thus improving the S/N with respect to a regular average or, more importantly, to lower resolution observations.

The same reduction and extraction procedures were used for the NIR and visible arms of X-Shooter, but the S/N in the small common wavelength interval between the two arms is low (about 1), which makes difficult to rescale the visible data to the NIR data scale. Since we have no z' detection of CFBDSIR2149, we cannot calibrate the visible spectrum on photometry. We therefore caution that this crude rescaling is probably inaccurate. Therefore, when NIR and visible spectra are shown together, their relative intensity before and after 1 μm is not reliable.

We checked the flux homogeneity of this large-wavelength coverage spectral data by calibrating it on our existing WIRCAM and NTT photometry (see Table 1). We synthetised the uncalibrated science spectrum colours by integrating them on WIRCam global transmission, including filter, instrument, and telescope transmission and the detector quantum efficiency (see Sect. 2.2 of Delorme et al. 2008b, for details) and determined a scaling factor for each of the broadband filter range so that the $YJHK_s$ Vega magnitudes derived for CFBDSIR1458AB spectrum would match those observed in broadband photometry. The resulting calibration factors are summarised in Table 3, showing that photometry and spectrophotometry agree within 1σ.

As shown in Table 3, we also derived spectrophotometric CH_{4on} and CH_{4off} magnitudes from the spectra. Since we do not have a parallax for CFBDSIR2149 yet, we can only derive colours from the spectra. We had to anchor these colours to the J-band photometry to obtain the spectrophotometric CH_{4on} CH_{4off} magnitudes in the WIRCam photometric system.

We used this X-Shooter spectrum to derive the spectral indices defined in Burgasser et al. (2006), Warren et al. (2007), and Delorme et al. (2008a) that trace the strength of several molecular absorption features typical of T dwarfs. As shown in Table 2, the atmospheric features are typical of a T7-T7.5 dwarf, with a significantly enhanced K/J index, telltale of a weak CIA (though the greenhouse effect could participate in K-band flux enhancement, see Allard & Homeier 2012), and therefore of a low-pressure photosphere (Leggett et al. 2002; Burgasser et al. 2004; Golimowski et al. 2004; Knapp et al. 2004; Burgasser et al. 2006). Hiranaka et al. (2012) propose an alternative explanation for the similarly red SED of some peculiar L dwarfs, which could be caused by a thin dust layer above the photosphere. Since most of the dust is condensated in late T dwarfs' photospheres, this alternative hypothesis is much weaker for objects as cool as CFBDSIR2149, making a lower than usual pressure in the photosphere the most likely hypothesis to explain the red $J - Ks$ colour of this object. Such low pressure can be the sign of a young, low-mass, and therefore low-gravity object and/or

Table 2. Value of the NIR spectral indices (as defined by Burgasser et al. 2006; Warren et al. 2007; Delorme et al. 2008a) for some of the latest known brown dwarfs.

Object	Sp. type	H_2O-J	W_J	CH_4-J	H_2O-H	CH_4-H	NH_3-H	CH_4-K	K/J
CFBDSIR2149	T7/T7.5	0.067	0.404	0.198	0.222	0.138	0706	0.133	0.199
		±0.003	±0.004	±0.004	±0.007	±0.006	±0.015	±0.023	±0.003
		T7.5	T7	T8	T7	T7.5	–	T6.5	–
SDSS1504+10	T7	0.082	0.416	0.342	0.241	0.184	0.668	0.126	0.132
Gl570D	T7.5	0.059	0.330	0.208	0.206	0.142	0.662	0.074	0.081
2M0415	T8	0.030	0.310	0.172	0.172	0.106	0.618	0.067	0.133
Ross458C	T8+	0.007	0.269	0.202	0.219	0.107	0.701	0.082	0.192
Wolf940B	T8+	0.030	0.272	0.030	0.141	0.091	0.537	0.073	0.111

Notes. Values were derived using spectra from this article and from Burgasser et al. (2006), Delorme et al. (2008a), Burningham et al. (2009, 2010).

Table 3. Photometry and spectrophotometry of CFBDSIR2149 (using WIRCam/MegaCam filter set to generate synthetic colours).

	z'_{ab}	Y	J	H	K_s	CH_{4off}	CH_{4on}
Photometry	>23.2	20.83 ± 0.09	19.48 ± 0.04	19.89 ± 0.11	19.35 ± 0.09	–	20.7 ± 0.25
Spectrophotometry[2]	24.51[1]	20.89[1]	Reference	19.98	19.43	19.35	20.89
Calibration factor[3]	–	–10%[1]	Reference	+8%	+8%	–	–

Notes. z' is in AB system, all others in Vega system. [(1)] Strong systematical uncertainties because of data rescaling below 1 μm. [(2)] Spectrophotometry is anchored on $J = 19.48 \pm 0.04$ from WIRCam photometric measurements. [(3)] Calibration factors are the factors to apply to the spectra in Y, J, H, and K bands so that it matches the broad band photometry.

of a more opaque, higher altitude photosphere typical of a high metallicity object.

Figure 3 presents a simple comparison of CFBDSIR2149 spectrum with BT-Settl atmosphere models from Allard et al. (2012) at different effective temperatures and gravity. Though we defer a more exhaustive analysis of the spectrum to a dedicated section, this first glance at our target's spectrum shows the following.

- Models at moderate gravity ($\log g \geq 4.5$) typical of relatively young, thin-disk objects aged 0.5−2 Gyr old (from stellar evolution models of Baraffe et al. 2003) cannot reproduce both the strong absorption bands in H-band and the enhanced flux in K-band. Trying to fit higher gravity models ($\log g$>5.0) to the observed spectrum leads to even worse matches.
- Models at the very low gravity ($\log g \sim 3.5$) typical of very young objects (1−20 Myr) predict a K-band (and H-band) flux enhancement that is much stronger than what we observe for CFBDSIR2149.
- Models at low gravity ($\log g \sim 3.75$−4.0) typical of intermediate-age objects (20−200 Myr) produce a SED relatively close to the observed spectrum.
- Models at temperatures higher than 800 K significantly underestimate the temperature sensitive CH_4 and H_2O absorption bands in the J and H bands, which are significantly weaker in models at temperatures higher than 800 K than they are in the observed spectrum. Conversely, they are too strong in models at a temperature cooler than 650 K.

4. Kinematic analysis: does CFBDSIR2149 belong to the young moving group AB Doradus?

4.1. Proper motion

We used the multi-epoch images described in the previous section to derive the proper motion of CFBDSIR2149. To improve our astrometric accuracy, we did not use the absolute positions of the source measured on each image, but calculated a relative local astrometric solution for each pair of first-epoch and second-epoch measurements. This was achieved by cross-matching first and second epochs and calculating the astrometric solution (using *Scamp*, Bertin 2006) of the second epoch using the first epoch image as the reference.

The most significant source of error was the centroid positioning error of this faint source, thus we used PSF-fitting with *Sextractor* to improve our accuracy. Given the very asymmetrical SED of late T dwarfs, another source of error is the atmospheric chromatic refraction (ACR, see e.g. Dupuy & Liu 2012). Since the flux barycentre in broad band filters is not at the same wavelength position for T dwarfs as it is for the background stars we used to derive the astrometric solution, ACR introduces a systematic shift in the centroid position. This depends mostly on the filter used and on the airmass at the time of the observations. This effect is relatively small in the NIR (a few mas, Albert et al. 2011), but we caution that our error estimates for proper motion measurements do not take this systematic error into account, so those errors represent lower limits. We also neglect parallax effects, which should be below 10 mas, given the photometric distance (35−50 pc) and our 28-month baseline between our first (13/08/2009) and our last (23/12/2011) epochs. According to Tinney et al. (2003) the bias from ACR is negligible in the J-band, therefore both the parallax effect and ACR effects are negligible compared to our measurement accuracy (~30 mas yr^{-1}), meaning the uncertainties are dominated by measurement errors and not by systematics for our J-band data. These proper motion measurements are given in Table 4, together with the least square linear fit of proper motion using the measurement of the position relative to the first epoch as input for each epoch. The fit was weighted at each epoch by the inverse of the error squared. Since we are only interested by the relative motion, we assumed the first-epoch measurement error to be infinitesimal and we attributed the full error of each

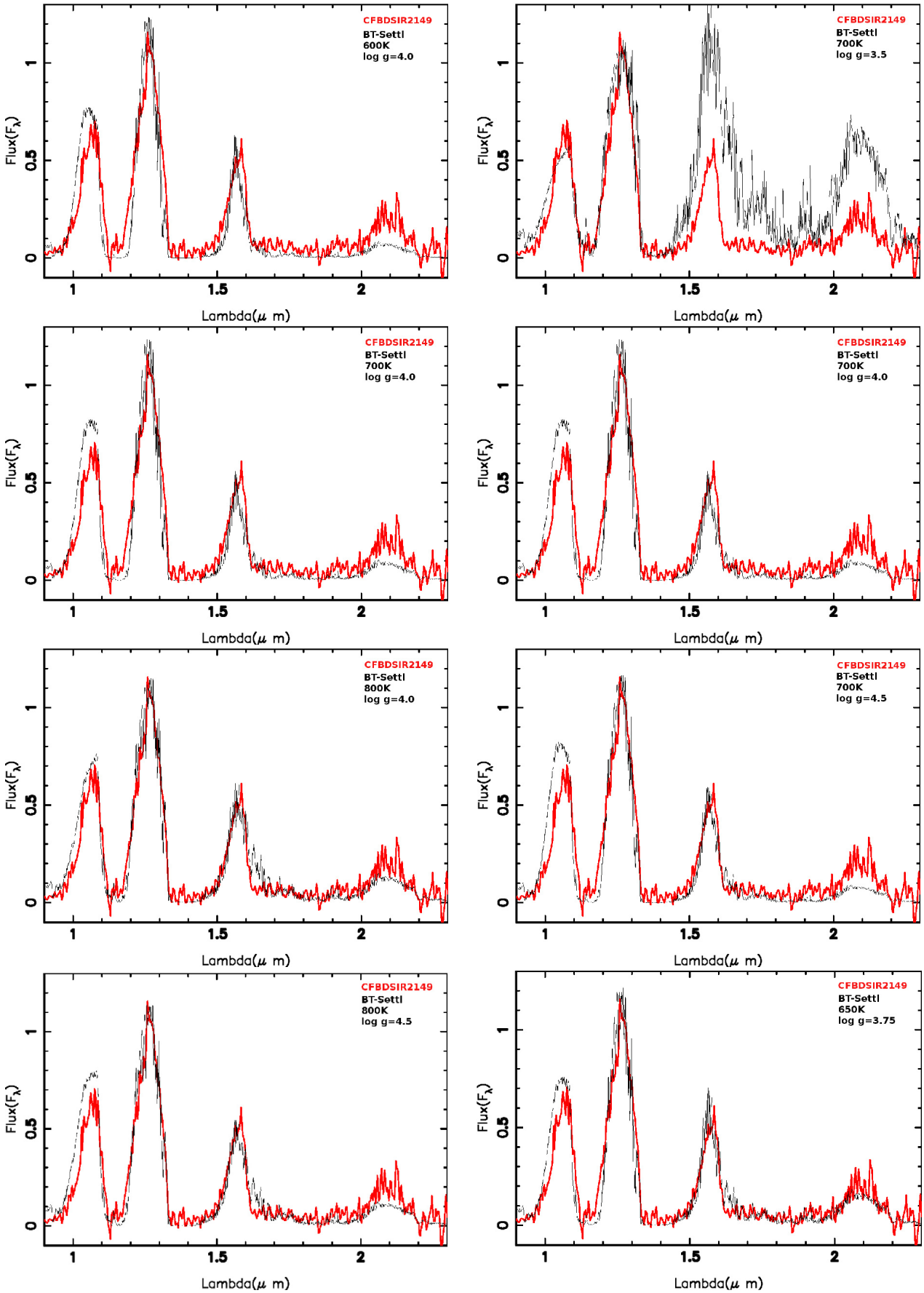

Fig. 3. Comparison of CFBDSIR2149 full spectrum at $R = 225$ with BT-Settl models of varying effective temperature (*left*) and gravity (*right*). Last row shows the models that agree best with J, H, K data for field gravity (*left*, $\log g = 4.5$ and $T_{\rm eff} = 800$ K) and free-floating planet gravity (*right*, $\log g = 3.75$ and $T_{\rm eff} = 650$ K).

Table 4. Proper motion measurement of CFBDSIR2149.

Epoch 1	Epoch 2	Proper motion (RA) $''$yr^{-1}	Proper motion (Dec) $''$yr^{-1}
$J_{13/08/09}$	$Js_{23/09/10}$	0.121 ± 0.042	–0.106 ± 0.044
$Js_{23/09/10}$	$J_{26/12/11}$	0.026 ± 0.070	–0.098 ± 0.088
$J_{13/08/09}$	$J_{26/12/11}$	0.067 ± 0.030	–0.104 ± 0.043
Weighted fit (J-band data)		0.085 ± 0.024	–0.105 ± 0.031
Weighted fit (all data)		0.081 ± 0.017	–0.124 ± 0.019

Notes. Discovery position (13/08/09) is RA: 21h49′47.2″ Dec: −04d03m08.9s.

epoch n − *epoch* 1 measurement to epoch n. The measurements using the other filter sets are much more dispersed, but as shown in Table 4, including all data in the fit decreases the fit measurement error, though the use of different filters should add small ACR systematics. In the following, we use the proper motion derived from the full data set, but caution that the error bar associated is a lower limit. A-contrario, the error we derived only on J-band data, with well controlled systematics and much less data, can be seen as a conservative upper limit of the error bars of the full data set.

4.2. Young moving group membership probability

Since the photometry and the spectrum of CFBDSIR2149 show tentative youth indicators, we have estimated the probabilities that this object is a member of several moving groups and associations (β-Pictoris, Tucana-Horologium, AB Doradus, TW Hydrae: Zuckerman et al. 2004; Columba, Carina, Argus, the Pleiades, ϵ Chameleontis, the Hyades, and Ursa Majoris: Torres et al. 2008), as well as a field member.

To do this, we used a Bayesian inference method that consists in answering the following question: given the XYZ galactic position and UVW space velocity of our object, as well as the distribution of equivalent quantities for each group and the field, what is the probability of it actually being a member of each group? The field and groups correspond to the different hypotheses, and in principle, the input parameters to such an analysis would be the XYZUVW for our object. However, we do not have a measurement for its radial velocity or its trigonometric distance. There is a standard way to deal with this that is generally called *marginalisation* over unknown parameters, consisting of repeating the analysis with several values for this parameter, then comparing the sum of the resulting probability densities for each hypothesis. For more details, we refer the reader to Feigelson & Jogesh Babu (2012) for a general description of Bayesian inference, as well as Malo et al. (2012) for an analysis similar in many ways to what we do here. We used the same XYZUVW distributions for each group and the field as described in Malo et al. (2012).

We highlight the three major differences between this analysis and ours: (1) we took the measurement errors on input parameters into account, by convolving each association's parameter distribution with a Gaussian of characteristic width corresponding to this error. (2) We treated distance and radial velocity as marginalised parameters, instead of just distance. (3) We took what is called the prior probability into account, which was set to unity in the work referred to. The value of this prior corresponds to the probability that our object is a member of a given group if we have absolutely no input data on the object. This is the simple ratio of the number of members in the group in question to the total number of stars we could have observed, reflecting the obvious fact that any random star had a much higher probability of belonging to the field than to any young association, since there are many more field stars than there are young association members. If this quantity is accurately estimated, it would ensure that 90% of members with 90% membership probability would be actual members. Without this prior, CFBDSIR2149 would have a 99.9% membership probability of belonging either the AB Doradus moving group (ABDMG) or to the β-Pictoris moving group (BPMG). Notably, the membership probability for ABDMG is very high because of the proximity of CFBDSIR to the ABDMG cinematic locus (see Fig. 4).

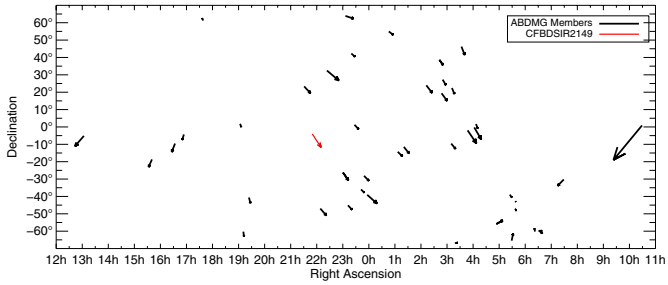

Fig. 4. Vectors representing the norm and direction of the proper motion of CFBDSIR2149 compared to the map of ABDMG members' proper motions.

To give a value to this prior for the young association hypotheses, we used the number of known young moving group members. For the field hypothesis, we used the fact our object is conservatively younger than 500 Myr since its spectrum is fairly indicative of an age in the 20 to 200 Myr range. Given that evolutionary and atmosphere models of young substellar objects are not yet fully reliable, we preferred to set a conservative upper age limit of 500 Myr. To inject this information into our Bayesian inference, we simply treated the prior as the ratio of stars in each moving group to the total population of field stars younger than 500 Myr that distant from 0 to 100 pc in a galactic disk simulation from the Besançon Galaxy model (Robin et al. 2003). We are confident this range of distances is reliable, since the young moving groups we considered lie within 100 pc of the Sun, and the photometric distance of our candidate is comfortably below 100 pc. This estimate is in fact quite conservative since it is generally accepted that the populations of young moving groups are still incomplete, meaning we might underestimate their respective membership probabilities. A third reason makes our membership probability conservative: when considering the field hypothesis we do not use the proper motion distribution of specifically young field objects, but of the general field population. Since young field objects have a narrower proper motion distribution (Robin et al. 2003), we therefore overestimate the field membership probability.

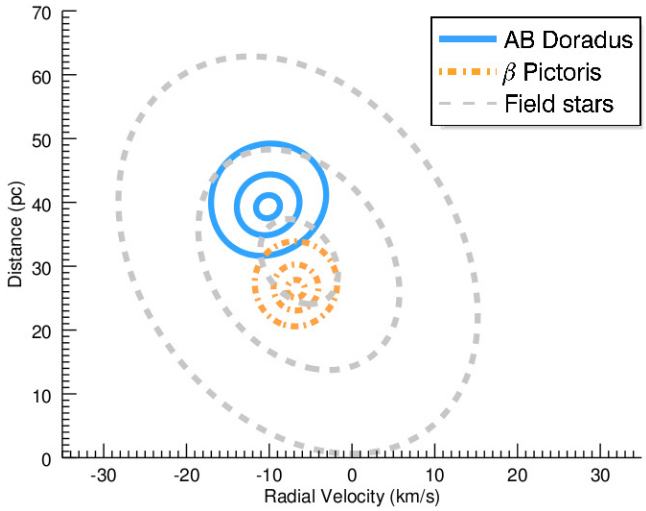

Fig. 5. Bayesian probability densities over distance and radial velocity derived from CFBDSIR2149 proper motion, for the 3 most probable membership hypotheses. The contours encircle 10%, 50%, and 90% of the probability density for each hypothesis, respectively.

With this Bayesian analysis that conservatively considers that young field stars are much more numerous than young association stars, we find CFBDSIR2149 has a membership probability of 79.4% for AB Doradus and 13.3% for the field. The third most likely hypothesis, a membership in the young moving group β Pictoris, has a 7.3% probability.

This makes CFBDSIR2149 a good candidate for the 50−120 Myr-old, solar metallicity, ABDMG-moving group (Zuckerman et al. 2004; Luhman et al. 2005; Ortega et al. 2007). The most likely values of the marginalised parameters (distance and radial velocity) for the most probable hypotheses (AB Doradus, field, and Beta Pictoris membership) are shown in Fig. 5. For the young field hypothesis, the Bayesian estimate provides a statistical (most likely) distance of 31 ± 13 pc and a radial velocity of -6 ± 9 km s^{-1}. According to the Allard et al. (2012) BT-Settl isochrones, the photometric distance of a 700 K, 500 Myr-old field brown dwarf with CFBDSIR brightness would be between 25 and 40 pc (respectively using the K_s and J-band photometry), in reasonable agreement with the Bayesian kinematic estimation. A younger age – our field prior is compatible with any age below 500 Myr – would lead to higher photometric distances and therefore to a more marginal agreement for the field hypothesis.

For the highest probability hypothesis, namely that our target belongs to ABDMG, the statistical distance is 40 ± 4 pc and the radial velocity is -10 ± 3 km s^{-1}. According to the Allard et al. (2012) BT-Settl isochrones, the photometric distance of a 700 K, 120 Myr-old brown dwarf with CFBDSIR brightness would be between 35 and 50 pc (respectively using the K_s and J-band photometry), which is in good agreement with the Bayesian estimation.

For the BPMG hypothesis the Bayesian estimate provides a statistical (most likely) distance of 27 ± 3 pc and a radial velocity of -7 ± 2 km s^{-1}. According to the Allard et al. (2012) BT-Settl isochrones, the photometric distance of a 650 K, 20 Myr-old field brown dwarf with CFBDSIR brightness would be between 25 and 35 pc (respectively using the K_s and J-band photometry), in reasonable agreement with the Bayesian kinematic estimation.

If we integrate the probability distribution of Fig. 5 over the photometric distance estimate range, we can obtain a membership probability that includes this information. We use the photometric distance estimate for the field for an age of 500 Myr, which is the closest to the field Bayesian estimate, and therefore slightly favours the field hypothesis. This yields a membership probability of 87% for the ABDMG, 7% for the BPMG, and 6% for the field. Also, since a fraction of field objects are younger than 150 Myr, the actual probability that CFBDSIR2149 is actually younger than 150 Myr is higher than its membership probability to ABDMG and BPMG. Taking that into account, *CFBDSIR2149 has a membership probability of 87% for the ABDMG, 7% for the BPMG, 3% for the young field (age < 150 Myr) and 3% for the field (150 Myr < age < 500 Myr).*

We caution that this introduces significant uncertainties into the calculation, because of the low reliability of photometric distance estimates. To assuage this concern, we derive in the following what could be seen as lower limits to ABDMG membership probability by looking at scenarios that are even more favourable to the field, using a prior that allows objects as old as 1 Gyr and 10 Gyr to be included in the prior. This is very conservative because the CFBDSIR2149 spectrum indicates a much younger age (<200 Myr, see previous section). With the prior including all field stars younger than 1 Gyr, this yields 72% membership probability to ABDMG, 22% to the field of all ages below 1 Gyr, and 6% to the BPMG, based on position and proper motion alone. If we integrate the Bayesian distance estimates on the photometric distance estimate ranges, we derive a membership probability of 83% for the ABDMG, 6% for the BPMG, 3% for the young field (age < 150 Myr), and 8% for the field (150 Myr < age < 1 Gyr). If we use the even more extreme prior including all field stars younger than 10 Gyr and integrate these probabilities on the photometric distance estimates (using a distance range of 20−35 pc for a 5 Gyr T7 dwarf), we still get 63% membership probability to ABDMG, 32% to the field of all ages below 10 Gyr, and 5% to the BPMG. As discussed in the previous section, the spectral features of this object are not compatible with an old age, unless it has a strongly super-solar metallicity. Since high-metallicity stars are rare, and are especially rare among old stars, using as the weight of our field hypothesis all stars below 10 Gyr is not a realistic hypothesis. Using this prior therefore does provide a very strong lower limit on the membership probability of CFBDSIR2149 in the ABDMG, but is not indicative of its actual membership probability.

Our Bayesian analysis that takes right ascension, declination, proper motions, and distance estimates into account allows setting the following constraints on the membership probability of CFBDSIR2149 to the ABDMG:

- an extremely conservative lower limit of 63% that we do not consider realistic,
- a very conservative lower limit of 83%,
- a conservative 87% membership probability of CFBDSIR2149 to the ABDMG, which we will use as our best estimate in the following.

We note that when including the possibility that CFBDSIR2149 is a field object younger than 150 Myr but unrelated to a known association, the overall probability that it is younger than 150 Myr is therefore higher than 95%. The following section explores the spectral properties of CFBDSIR2149, assuming that it is indeed younger than 150 Myr.

Finally, as a sanity check, we determined whether another CFBDS brown dwarf, CFBDSIR1458, described in

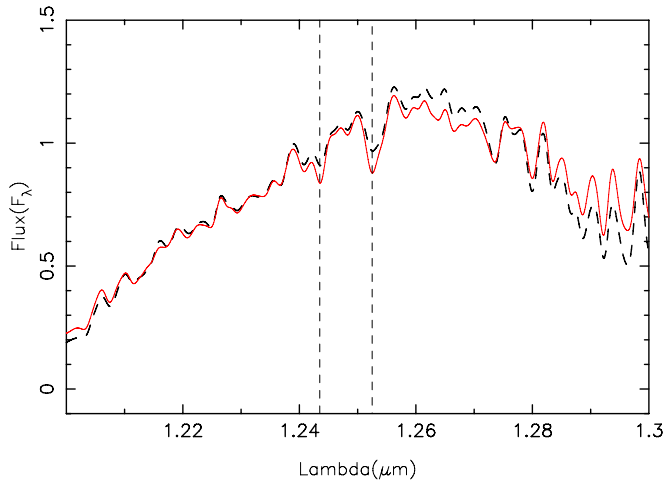

Fig. 6. Comparison of BT-Settl 2012 models at the same temperature (700 K), but with different gravity (red: log g = 3.5, black: log g = 4.5). The KI doublet position is highlighted by the dashed lines.

Delorme et al. (2010) as an old brown dwarf on the grounds of its spectral features, could turn out to be a young moving group member using the same kinematic analysis. The result is a 100% probability that this object belongs to the field, with the probability of belonging to any young moving group lower than 10^{-20}, even using the 500 Myr prior, which is more favourable to young moving group membership. These kinematic results are therefore in excellent agreement with the spectral analysis by Delorme et al. (2010) and Liu et al. (2011) that identify CFBDSIR1458 as an old field brown dwarf.

5. Physical properties of CFBDSIR2149

5.1. Comparison to other late T dwarfs

A direct comparison of CFBDSIR2149's spectrum with the spectra of other T7-T8.5 brown dwarfs (see Fig. 8) clearly shows its enhanced K-band flux. The spectrum of CFBDSIR2149 shows another low-gravity feature, namely the enhanced absorption by the 1.25 μm potassium doublet (see Fig. 6). According to Allard & Homeier (2012), the strength of the doublet in the spectra depends both on the abundance of potassium in the atmosphere and on the strength of the CH_4 and H_2O absorption bands that shape the pseudo-continuum through which the doublet forms. At T dwarf temperatures, a lower gravity increases the doublet strength by playing on each of these parameters: the pseudo-continuum is weakened at low gravity for a given effective temperature, while the potassium abundances tends to increase because of enhanced vertical mixing effects in low-gravity atmospheres. The same trend has been empirically observed in the T dwarf by Knapp et al. (2004).

This doublet decreases in strength from T4 to T7, until it totally disappears on regular field dwarfs later than T7 (Knapp et al. 2004), and should be almost absent from the T7/T7.5 spectrum of CFBDSIR2149 if it had field gravity and solar metallicity. The comparison with the T7 2M0727+1710 (see Fig. 7), which has already been identified as a low-gravity T7 by Knapp et al. (2004) illustrates that the KI absorption doublet is more prominent in CFBDSIR2149.

Another interesting object to compare with is the very red T8.5 brown dwarf Ross458C (Scholz 2010; Goldman et al. 2010; Burgasser et al. 2010; Burningham et al. 2011a), which

Table 5. Colours of CFBDSIR2149 and Ross458C.

	$Y-J$	$J-H$	$J-K_s$	$H-K_s$
CFBDSIR2149	1.35 ± 0.09	–0.41 ± 0.11	0.13 ± 0.09	0.54 ± 0.14
Ross458C	1.52 ± 0.02	–0.38 ± 0.03	0.08 ± 0.03	0.46 ± 0.04

presents a K-band flux excess comparable to what we observe for CFBDSIR2149. As discussed in Burgasser et al. (2010) and Burningham et al. (2011a), this object shows many features of low gravity, and it belongs to a young stellar system (150−800 Myr), with a metallicity that is slightly higher than solar ([Fe/H] ∼ 0.2−0.3).

Before we engage in a closer comparison between CFBDSIR2149 and Ross458C, we have to point out that since CFBDSIR2149 appears slightly warmer than Ross458C, it should have a redder $J-K_s$ (see Fig. 2) and a higher J/K spectral index, because of effective temperature alone. This makes the direct comparison of these gravity-sensitive features difficult: they are slightly stronger in CFBDSIR2149 but this difference, including the presence of the 1.25 μm potassium doublet, might be fully accounted for by the difference in effective temperature rather than by an even lower gravity. To compare the colours of both objects using the same photometric system, we calculated the NIR colours of Ross458C in the WIRCam filter system using the spectra provided by Burningham et al. (2011a). The resulting colours are shown in Table 5 and are very similar to those observed for CFBDSIR2149. The $J-K$ colour of Ross458C with WFCAM filter system is much bluer (−0.25, Burningham et al. 2011b) because the atypical K-band filter used on WFCAM cuts a significant part of T dwarf flux bluewards of 2 μm and extends redwards of 2.3 μm where late T dwarfs have no flux left.

Because of the degeneracy between effects of low gravity and high metallicity, the similar colours and spectral features of CFBDSIR2149 with respect to Ross458C can be explained either by a similar age/[M/H] combination or by a younger age and a more common solar metallicity for CFBDSIR2149. There is also the possibility that CFBDSIR2149 is older and has an even higher metallicity than Ross458C, but this is much less probable both because of its kinematics and because of the scarcity of significantly over-metallic stellar systems (only ∼4% of stars have metallicity >0.3, Santos et al. 2005). Given the probable association of CFBDSIR2149 to the 50−120 Myr AB Doradus moving group, the hypothesis that it is a slightly warmer, slightly younger solar metallicity counterpart of Ross458C is most likely, especially because it is also consistent with the [M/H] = −0.02 ± 0.02 metallicity distribution derived by Ortega et al. (2007) for ABDMG members. According to the Lyon stellar evolution models of Baraffe et al. (2003), at solar metallicity, such a 650−750 K brown dwarf aged 50 Myr has a mass of four to five Jupiter masses and a log g of about 3.9. This would make CFBDSIR2149 a "free-floating planet", with the same atmospheric properties as any 50 Myr-old, 4−5 $M_{\rm Jup}$, T-type exoplanet, which makes it an invaluable benchmark for exoplanet atmosphere studies. In case we adopted the higher age hypothesis of 120 Myr (Luhman et al. 2005; Ortega et al. 2007), the conclusion would be similar, CFBDSIR2149 then being a 120 Myr-old, 6−7 $M_{\rm Jup}$ free-floating planet with a log g of ∼4.1.

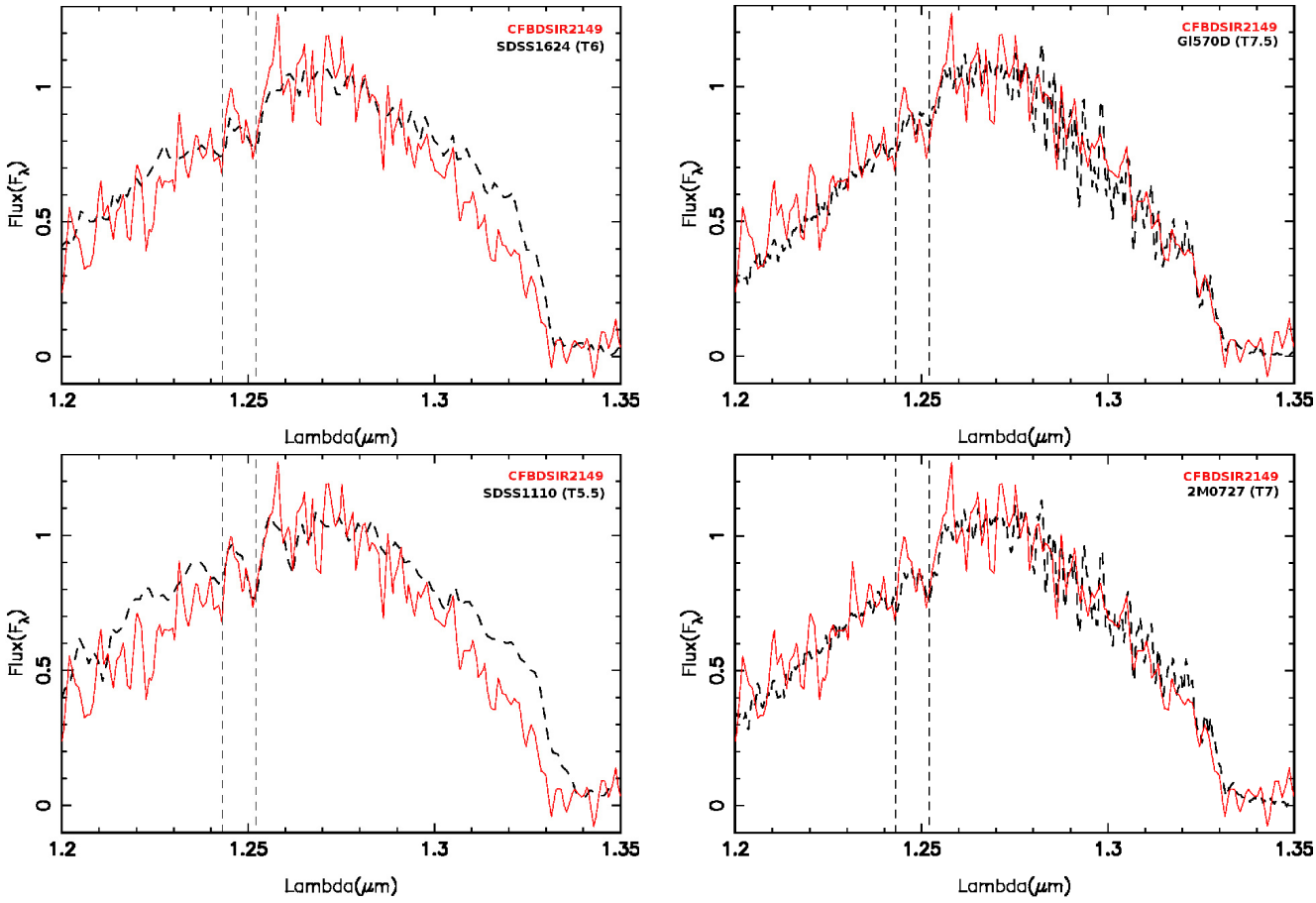

Fig. 7. Comparison of CFBDSIR2149 spectrum (red) in the *J* band, with low gravity (*bottom*, Leggett et al. 2002; McLean et al. 2003), regular (*top*, Strauss et al. 1999; McLean et al. 2003) T6 (*left*) and T7 (*right*) brown dwarfs (black). The dashed line indicates the position of the potassium doublet.

5.1.1. Revisiting Ross458C

The young age hypothesis for Ross458C is supported by the fast rotation (11 km s^{-1}; Donati et al. 2008) observed for its primary M1 star Ross458A. The corresponding upper limit of the period (when the projected rotational speed $V \sin(i) = V$, the equatorial rotation speed) of ~2.5 days. Delorme et al. (2011) established that early M dwarfs in the Hyades and Praesepe have already converged toward a clean mass-period relation. Gyrochronology (Barnes 2003) therefore allows asserting that almost all early M dwarfs that rotate faster than the 12 to 14 days observed in the early M dwarfs of these ~600 Myr clusters are younger than the cluster themselves. The exceptions are the few stars that have experienced significant angular momentum transfer from orbital momentum to rotational momentum through close tidal interactions within a multiple system. Since Ross458A has a rotation period that is much shorter than 12−14 days, and is not known as a very close dynamically interacting binary, we can safely deduce that the Ross458 system is younger than 600 Myr. This upper age limit is more stringent than the 800 Myr upper age limit from Burgasser et al. (2010), and it is consistent with the 200−300 Myr derived from the spectral analysis of Ross458C and CFBDSIR2149.

Given the probable higher metallicity and lower temperature of Ross458C, the gravity of both objects should be similar. Because of the fast cooling down of a substellar object during its first few hundred Myr, a gravity within 0.2 dex. of CFBDSIR2149 for the 650−700 K Ross458C is only compatible with an age lower than 200 Myr (300 Myr if we use the older age estimate for the AB Doradus moving group), with a corresponding maximum mass of 8 $M_{\rm Jup}$ (respectively 10). These rough estimates, also compatible with the age value from Burgasser et al. (2010), would redefine the T8.5 brown dwarf Ross458C as an exoplanet orbiting the Ross458 stellar system, if we follow the controverted International Astronomical Union official definition of a planet, even if its formation mechanisms are probably more akin to the formation of multiple systems. Indeed, the formation of Ross458 through planetary formation scenarii, such as core accretion or gravitational instability, is unlikely both because of the very large separation (1200 AU, Scholz 2010) and the low mass of the M1 primary Ross458A.

5.2. Comparison to models

We used several sets of models to match the observed spectra of CFBDSIR2149. The corresponding plots are shown in Fig. 3 (BT-Settl models) and Fig. 9, and include planetary atmosphere models meant for the HR8799 planets Currie et al. (2011) adapted from Burrows et al. (2003, hereafter referred to as BSL03) and from Madhusudhan et al. (2011, hereafter referred to as MBC20111), as well as the BT-Settl-models.

We did not attempt a numerical fit of our observed spectra to these various models grids because of the strong (and model-dependent) systematics uncertainties in atmosphere models, notably missing CH_4 absorption lines bluewards of 1.6 μm whose lack is obvious in Fig. 9, including right of the *H*-band peak.

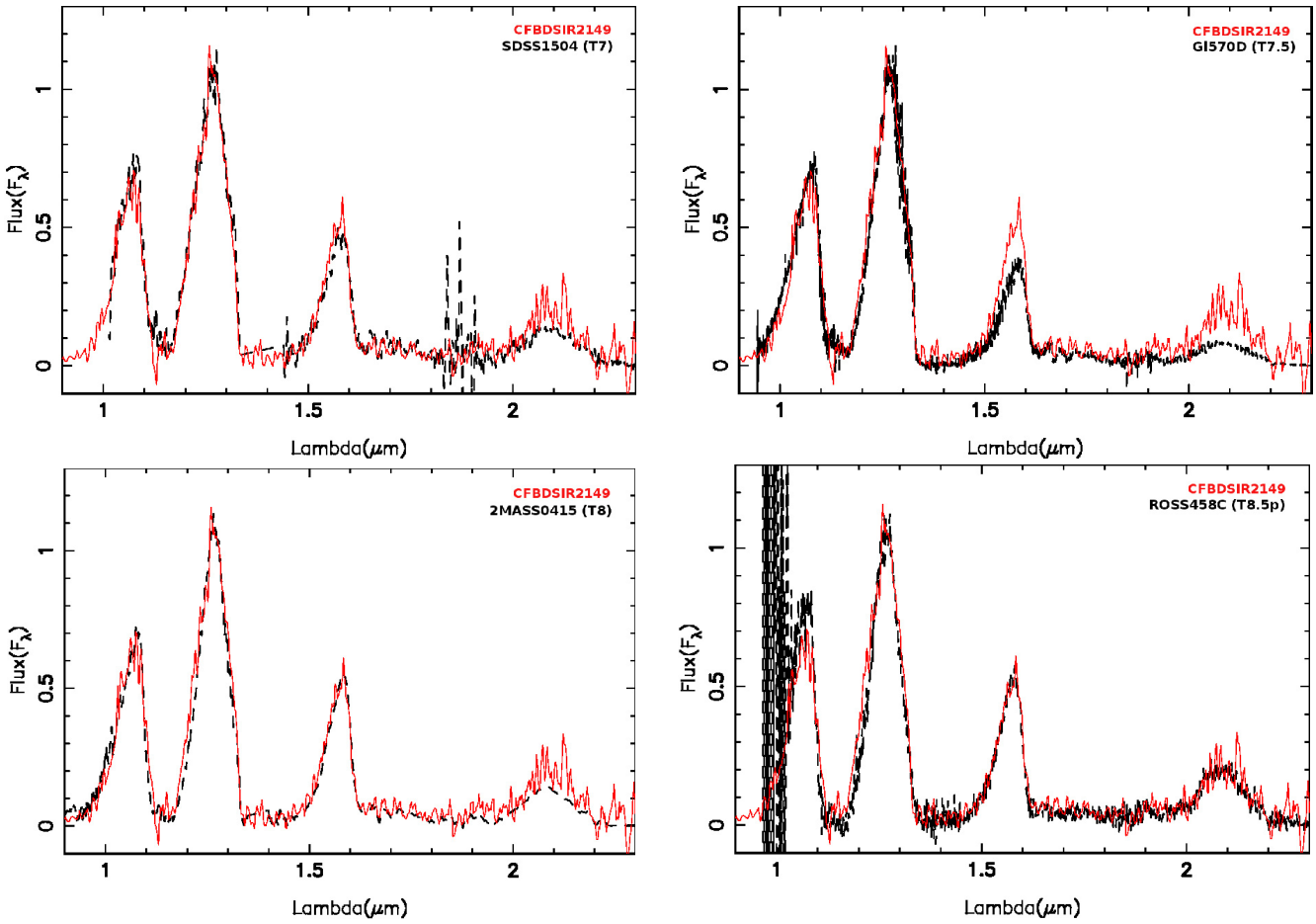

Fig. 8. Comparison of CFBDSIR2149 spectrum with other late T dwarfs. Spectra have been taken from McLean et al. (2003), Burgasser et al. (2003), Chiu et al. (2006), and Burningham et al. (2011b).

We preferred matching models visually, rather than injecting ad-hoc restrictions in a fit by artificially weighting out parts of the models we suppose are affected by systematics. Discussing the resulting numerical values of such a fit would not be more relevant than discussing the models that visually match the observed spectrum and would unfairly hide some of the limitations that come with comparing poorly constrained models and poorly sampled model grids to noisy data.

The main difficulty matching CFBDSIR2149 spectrum is to find a model that correctly reproduces both its very deep CH_4 absorption in the H-band and its strongly enhanced K-band flux. The former is easily matched by all models with cool (700 K) temperatures and relatively high gravities ($\log g$ = 4.5−5.0; see Fig. 9) while the latter can be matched by warmer, low-gravity models (see Fig. 8), but the combination of both is difficult to reproduce. The MBC models with clouds of types "A", "AE" and "AEE" very significantly fail to reproduce the SED of CFBDSIR2149 (see the "A" case on the lower right panel of Fig. 9), because they predict an extremely red NIR SED, due to their very thick cloud layers. In the "A" case, the cloud model includes no upper cloud boundary at all, i.e. no dust sedimentation effects of any kind, corresponding to the simplified cases of fully cloudy atmospheres like the AMES-Dusty models. The "E" models by comparison implement a steeply decreasing condensate density above a certain pressure level given as a model parameter, and can thus be tuned to produce clouds comparable to the BT-Settl models or the Marley & Saumon models for a certain $f_{\rm sed}$. As seen in Fig. 9 these "E" cloud models, as well as the BSL2003 and BT-Settl models offer a decent match to the spectrum when using relatively cool temperatures (650−700 K) to depress the H-band flux and relatively low gravities ($\log g$ = 3.75−4.1) to enhance the K-band flux, but all models suffer from missing CH_4 lines bluewards of 1.6 μm. This systematic shortcoming acknowledged, comparison with models gives a temperature of 650−750 K and a $\log g$ of 3.75 to 4.1 for CFBDSIR2149. BT-Settl models favour a cool 650 K, $\log g$ = 3.75 value that would only be compatible, according to the Baraffe et al. (2003) substellar evolution models, with the hypothesis that our target is a member of the 12 Myr-old β-Pictoris moving group, and with ABDMG membership, but only for its youngest age estimate (50 Myr; Zuckerman et al. 2004). Conversely, the ages derived from the MBC2011 "E" cloud models and BSL2003 models (also using Baraffe et al. 2003 models to translate temperature and gravity into age and mass) would be fully compatible with the probable (>95%) hypothesis that CFBDSIR2149 is younger than 150 Myr. Even in the extreme hypothesis that this object were aged 500 Myr, its mass (11 $M_{\rm Jup}$) would still be below the deuterium burning mass of 13 $M_{\rm Jup}$ that serves as an artificial limit between planets and brown dwarfs. According to this mass-driven definition, CFBDSIR could be called an IPMO or a free-floating planet.

A major conclusion we can draw from these comparisons is that CFBDSIR2149's spectrum is close to the standard BT-Settl and BSL2003 models and can be matched without using the

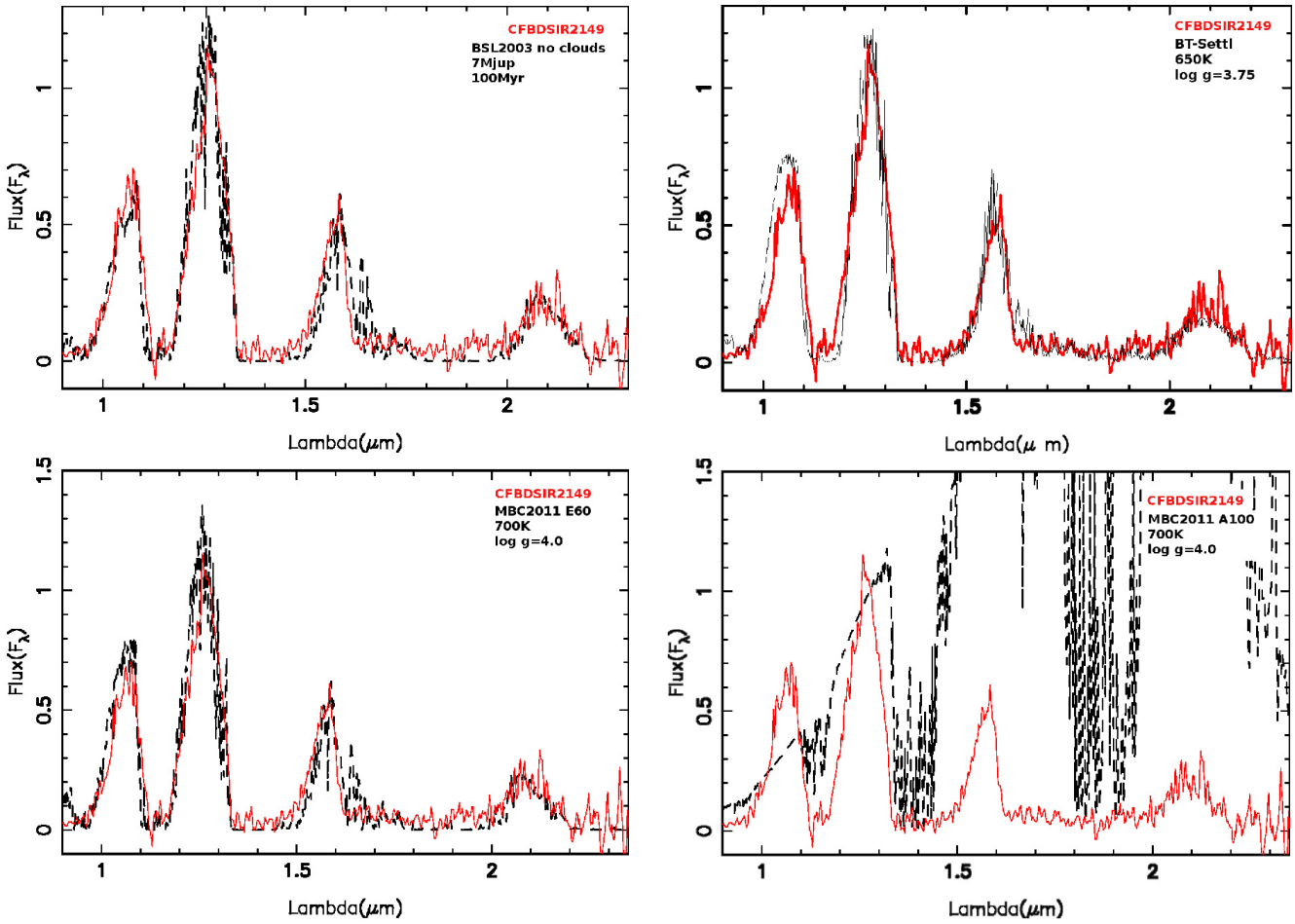

Fig. 9. Comparison of CFBDSIR2149 full spectrum at $R = 225$ (red) with various models (black). *Upper left*: Burrows Sudarsky Lunine 2003 model for a 100 Myr, 7 $M_{\rm jup}$ planet (i.e. $T_{\rm eff} \sim 750$ K, $\log g \sim 4.1$) with no clouds. *Upper right*: BT-Settl models for $T_{\rm eff} = 650$ K and $\log g = 3.75$. *Lower left*: Madhusudhan et al. (2011) cloudy "E" model at $T_{\rm eff} = 700$ K, log = 4.0 and 60 μm enstatite particles in clouds. *Lower right*: Madhusudhan et al. (2011) cloudy "A" model at $T_{\rm eff} = 700$ K, log = 4.0 and 100 μm particles in clouds.

thick-cloud models that have been created to account for the peculiar SED of the young exoplanets orbiting HR8799 (Currie et al. 2011). Given the very high dependence of the modelled SED on the type of cloud in these MBC2011 models (see the completely different SED modelled in the last row of Fig. 9, for the same gravity and temperature but with a different cloud parameter setting), that one of the cloud settings matches the observed spectrum at some point on the gravity/temperature grid as well the BT-Settl or BSL2003 models do is not surprising. Burningham et al. (2011a) also concludes that such adaptable cloud models were not necessary to account for Ross458C's spectrum, which can be fitted with BT-Settl models that use a self-consistent cloud model over their full parameter range.

If CFBDSIR2149 is indeed a 4−7 $M_{\rm Jup}$ ABDMG member, this would mean that the similar cool exoplanets of late T type targeted by upcoming high-contrast imaging instruments should have a spectrum closer to the model prediction than the heavier/warmer HR8799 planets of early T type. This would not be surprising, since the L/T transition atmospheres are known to be much more difficult to model than late T atmospheres for field brown dwarfs. Our results suggest the same is true at low gravity and that model predictions of the cool, low-mass exoplanets still to be discovered could in fact be more accurate than model predictions of the few warmer L/T transition exoplanets we already know.

6. Discussion

The ability to anchor the age and metallicity of CFBDSIR2149 through its probable membership in the AB Doradus moving group allowed us to constrain its gravity and effective temperature with atmosphere models and directly corroborate these conclusions through substellar evolution models. Comparison of the spectra to the solar metallicity atmosphere models points towards a 650−750 K atmosphere with a $\log g$ of 3.75−4.1. Using the stellar evolution models of Baraffe et al. (2003), these parameters translate into a 20 Myr to 200 Myr-old, 2 $M_{\rm Jup}$ to 8 $M_{\rm Jup}$, free-floating planet. These values are therefore fully compatible with the age range and properties of the AB Doradus moving group, even though ABDMG membership strongly favours the higher mass estimate and hint, in qualitative agreement with the claim of Burningham et al. (2011a), that BT-Settl models underestimate the K-band flux of late T dwarfs, resulting in slightly underestimating the gravity, masses, and ages of the observed T dwarfs (see Table 5). However our age and metallicity constraints do confirm that CFBDSIR2149 is a low-gravity, low-mass object, though not as extreme as the BT-Settl models alone would have implied. If its ABDMG membership is confirmed, this object would be a 4 to 7 $M_{\rm Jup}$ T-type free-floating planet.

That the spectrum of this probable intermediate age free-floating planet is relatively well modelled by standard atmosphere models – with no need of any ad-hoc injection of

thick clouds – hints that models would be more accurate for the cool (~700 K), lower mass, late-T exoplanets than for the warmer, L/T transition exoplanets, such as HR8799bcde (~900−1400 K). If CFBDSIR2149 ABDMG membership is confirmed, this would show that at temperatures cooler than the L/T transition, the overall NIR spectrum of late T objects does show low-gravity features but is not dramatically different to a field late T spectrum. Bowler et al. (2012) and Wahhaj et al. (2011) studied an L0 (1RXS J235133.3+312720B) and an L4 (CD-35 2722B) brown dwarf companions to AB Doradus members and similarly concluded that, for temperatures higher than the L/T transition this time, these objects had clear low-gravity features but that their overall SED was not dramatically different from early field L dwarfs. It therefore appears that by the age of AB Doradus the most problematic spectral range is the L/T transition, and that outside this range substellar objects exhibit a spectral energy distribution that is similar to that of field brown dwarfs and standard model predictions. This would confirm the detection capability hypotheses used to design the upcoming SPHERE and GPI planet imager instruments, at least for such intermediate ages.

Comparison of CFBDSIR2149 with Ross458C, has shown that both are probably young planetary mass objects. Since this analysis strongly favours the young age hypothesis of Ross458C, we can expect some kind of cascade effect leading to a downward revision of the age (and therefore mass) estimates of a fraction of the late T dwarf population. Indeed, even if CFBDSIR2149 and Ross458C are probably the youngest T dwarfs currently identified, their gravity sensitive features do not widely differ from some other known field T dwarfs. Many discovered late T dwarfs (see for instance Knapp et al. 2004; Burgasser et al. 2006; Lucas et al. 2010; Burningham et al. 2011b; Liu et al. 2011) have long been classified with low gravity ($\log g \leq 4.5$). Since these estimates were only grounded on the comparison of their spectra and colours to atmosphere models that have not been observationally constrained in this temperature and gravity range, the resulting planetary mass estimates have been seen as improbable lower limits. Our results hint that many of these low-gravity late T dwarfs would actually reside below the deuterium-burning mass. This supports the hypothesis that a small but significant fraction of the known population of late T dwarfs are free-floating planets, perhaps the visible counterpart of the free-floating planet population detected by microlensing by Sumi et al. (2011) and Strigari et al. (2012).

The conclusions for stellar and planetary formation models would also be far reaching. Either the planetary mass-field brown dwarfs are mostly the result of a stellar formation process, which would confirm that the fragmentation of a molecular cloud can routinely form objects as light as a few Jupiter masses, or these objects are mostly ejected planets. In this case, given that massive planets are less easily ejected from their original stellar system than lower mass ones, and that lighter planets are much more common than heavier ones (see Bonfils et al. 2012, for instance), this would mean free-floating, frozen-down versions of Jupiters, Neptunes, and perhaps Earths are common throughout the Milky Way interstellar ranges.

However, these speculations need the confirmation of CFBDSIR2149 as a member of ABDMG moving group to become robust hypotheses. Our ongoing parallax measurement programme for CFBDSIR2149 will improve the proper motion measurement and determine its precise distance, which should ascertain whether it is an ABDMG member. It will also bring strong constraints on the absolute flux and on the radius of CFBDSIR2149, enabling it to be used as a well-characterised benchmark for young late T dwarfs and the T-type, Jupiter-masses exoplanets that are likely to be discovered by the upcoming SPHERE, GPI, and HiCIAO instruments.

Acknowledgements. Based on observations obtained with MegaPrime/MegaCam, a joint project of CFHT and CEA/DAPNIA, at the Canada-France-Hawaii Telescope (CFHT), which is operated by the National Research Council (NRC) of Canada, the Institut National des Sciences de l'Univers of the Centre National de la Recherche Scientifique (CNRS) of France, and the University of Hawaii. This work is based in part on data products produced at TERAPIX and the Canadian Astronomy Data Centre as part of the Canada-France-Hawaii Telescope Legacy Survey, a collaborative project of the NRC and CNRS. This research has made use of the NASA/IPAC Infrared Science Archive, which is operated by the Jet Propulsion Laboratory, California Institute of Technology, under contract with the National Aeronautics and Space Administration. We acknowledge financial support from the "Programme National de Physique Stellaire" (PNPS) of the CNRS/INSU, France.

References

Albert, L., Artigau, É., Delorme, P., et al. 2011, AJ, 141, 203
Allard, F., & Homeier, D. 2012, Mem. Soc. Astron. It., submitted [arXiv:1206.1021]
Allard, F., Homeier, D., & Freytag, B. 2012, Roy. Soc. London Philos. Trans. Ser. A, 370, 2765
Allers, K. N., Liu, M. C., Dupuy, T. J., & Cushing, M. C. 2010, ApJ, 715, 561
Artigau, É., Lafrenière, D., Doyon, R., et al. 2011, ApJ, 739, 48
Baraffe, I., Chabrier, G., Barman, T. S., Allard, F., & Hauschildt, P. H. 2003, A&A, 402, 701
Barnes, S. A. 2003, ApJ, 586, 464
Bate, M. R. 2009, MNRAS, 392, 590
Bertin, E. 2006, in Astronomical Data Analysis Software and Systems XV, eds. C. Gabriel, C. Arviset, D. Ponz, & S. Enrique, ASP Conf. Ser., 351, 112
Bertin, E. 2010, in Astrophysics Source Code Library, record ascl.1010.068, 10068
Bertin, E., & Arnouts, S. 1996, A&AS, 117, 393
Bertin, E., Delorme, P., & Bouy, H. 2012, in AstrOmatic Software in the Era of Large Stellar Photometric Surveys, eds. A. Moitinho, & J. Alves, 71
Beuzit, J.-L., Feldt, M., Dohlen, K., et al. 2008, in SPIE Conf. Ser., 7014
Bonfils, X., Delfosse, X., Udry, S., et al. 2012, A&A, in press, DOI: 10.1051/0004-6361/201014704
Boss, A. P., Basri, G., Kumar, S. S., et al. 2003, in Brown Dwarfs, ed. E. Martín, IAU Symp., 211, 529
Bowler, B. P., Liu, M. C., Shkolnik, E. L., et al. 2012, ApJ, 753, 142
Burgasser, A. J., Kirkpatrick, J. D., Burrows, A., et al. 2003, ApJ, 592, 1186
Burgasser, A. J., Kirkpatrick, J. D., Lepine, S., et al. 2004, in AAS Meeting Abstracts, 205
Burgasser, A. J., Geballe, T. R., Leggett, S. K., Kirkpatrick, J. D., & Golimowski, D. A. 2006, ApJ, 637, 1067
Burgasser, A. J., Simcoe, R. A., Bochanski, J. J., et al. 2010, ApJ, 725, 1405
Burgess, A. S. M., Moraux, E., Bouvier, J., et al. 2009, A&A, 508, 823
Burningham, B., Pinfield, D. J., Leggett, S. K., et al. 2008, MNRAS, 391, 320
Burningham, B., Pinfield, D. J., Leggett, S. K., et al. 2009, MNRAS, 395, 1237
Burningham, B., Leggett, S. K., Lucas, P. W., et al. 2010, MNRAS, 404, 1952
Burningham, B., Leggett, S. K., Homeier, D., et al. 2011a, MNRAS, 414, 3590
Burningham, B., Lucas, P. W., Leggett, S. K., et al. 2011b, MNRAS, 414, L90
Burrows, A., Sudarsky, D., Lunine, J. I., et al. 2003, ApJ, 596, 587
Chauvin, G., Lagrange, A.-M., Dumas, C., et al. 2004, A&A, 425, L29
Chiu, K., Fan, X., Leggett, S. K., et al. 2006, AJ, 131, 2722
Cruz, K. L., Kirkpatrick, J. D., & Burgasser, A. J. 2009, AJ, 137, 3345
Currie, T., Burrows, A., Itoh, Y., et al. 2011, ApJ, 729, 128
Cushing, M. C., Kirkpatrick, J. D., Gelino, C. R., et al. 2011, ApJ, 743, 50
Cutri, R. M., Skrutskie, M. F., van Dyk, S., et al. 2003, 2MASS All Sky Catalog of point sources
Delorme, P., Delfosse, X., Albert, L., et al. 2008a, A&A, 482, 961
Delorme, P., Willott, C. J., Forveille, T., et al. 2008b, A&A, 484, 469
Delorme, P., Albert, L., Forveille, T., et al. 2010, A&A, 518, A39
Delorme, P., Collier Cameron, A., Hebb, L., et al. 2011, MNRAS, 413, 2218
Devillard, N. 2001, in Astronomical Data Analysis Software and Systems X, eds. F. R. Harnden, Jr., F. A. Primini, & H. E. Payne, ASP Conf. Ser., 238, 525
Donati, J.-F., Morin, J., Petit, P., et al. 2008, MNRAS, 390, 545
Dupuy, T. J., & Liu, M. C. 2012, ApJS, 201, 19
Faherty, J. K., Rice, E. L., Cruz, K. L., Mamajek, E. E., & Núñez, A. 2012, AJ, submitted [arXiv:1206.5519]
Feigelson, E. D., & Jogesh Babu, G. 2012 [arXiv:1205.2064]

Fukugita, M., Ichikawa, T., Gunn, J. E., et al. 1996, AJ, 111, 1748
Goldman, B., Marsat, S., Henning, T., Clemens, C., & Greiner, J. 2010, MNRAS, 405, 1140
Golimowski, D. A., Leggett, S. K., Marley, M. S., et al. 2004, AJ, 127, 3516
Graham, J. R., Macintosh, B., Doyon, R., et al. 2007, in BAAS 39, AAS Meeting Abstracts, 134.02
Haisch, Jr., K. E., Barsony, M., & Tinney, C. 2010, ApJ, 719, L90
Hiranaka, K., Cruz, K., & Marley, M. 2012, in AAS Meeting Abstracts, 219, 345.29
Hodapp, K. W., Suzuki, R., Tamura, M., et al. 2008, in SPIE Conf. Ser., 7014
Knapp, G. R., Leggett, S. K., Fan, X., et al. 2004, AJ, 127, 3553
Leggett, S. K., Hauschildt, P. H., Allard, F., Geballe, T. R., & Baron, E. 2002, MNRAS, 332, 78
Liu, M. C., Delorme, P., Dupuy, T. J., et al. 2011, ApJ, 740, 108
Lucas, P. W., Tinney, C. G., Burningham, B., et al. 2010, MNRAS, 408, L56
Luhman, K. L., Stauffer, J. R., & Mamajek, E. E. 2005, ApJ, 628, L69
Luhman, K. L., Burgasser, A. J., & Bochanski, J. J. 2011, ApJ, 730, L9
Madhusudhan, N., Burrows, A., & Currie, T. 2011, ApJ, 737, 34
Mainzer, A., Cushing, M. C., Skrutskie, M., et al. 2011, ApJ, 726, 30
Malo, L., Doyon, R., Lafrenière, D., et al. 2012, ApJ, accepted [arXiv:1209.2077]
Marois, C., Macintosh, B., Barman, T., et al. 2008, Science, 322, 1348
Marois, C., Zuckerman, B., Konopacky, Q. M., Macintosh, B., & Barman, T. 2010, Nature, 468, 1080
Marsh, K. A., Kirkpatrick, J. D., & Plavchan, P. 2010, ApJ, 709, L158
McLean, I. S., McGovern, M. R., Burgasser, A. J., et al. 2003, ApJ, 596, 561
Modigliani, A., Goldoni, P., Royer, F., et al. 2010, in SPIE Conf. Ser., 7737
Moeckel, N., & Veras, D. 2012, MNRAS, 422, 831
Moorwood, A., Cuby, J., & Lidman, C. 1998, The Messenger, 91, 9
Ortega, V. G., Jilinski, E., de La Reza, R., & Bazzanella, B. 2007, MNRAS, 377, 441
Peña Ramírez, K., Zapatero Osorio, M. R., Béjar, V. J. S., Rebolo, R., & Bihain, G. 2011, A&A, 532, A42
Peña Ramírez, K., Béjar, V. J. S., Zapatero Osorio, M. R., Petr-Gotzens, M. G., & Martín, E. L. 2012, ApJ, 754, 30
Puget, P., Stadler, E., Doyon, R., et al. 2004, in SPIE Conf. Ser. 5492, eds. A. F. M. Moorwood, & M. Iye, 978
Robin, A. C., Reylé, C., Derrière, S., & Picaud, S. 2003, A&A, 409, 523
Santos, N. C., Israelian, G., Mayor, M., et al. 2005, A&A, 437, 1127
Scholz, A., Jayawardhana, R., Muzic, K., et al. 2012, ApJ, 756, 24
Scholz, R.-D. 2010, A&A, 515, A92
Stamatellos, D., Maury, A., Whitworth, A., & André, P. 2011, MNRAS, 413, 1787
Strauss, M. A., Fan, X., Gunn, J. E., et al. 1999, ApJ, 522, L61
Strigari, L. E., Barnabè, M., Marshall, P. J., & Blandford, R. D. 2012, MNRAS, 2972
Sumi, T., Kamiya, K., Bennett, D. P., et al. 2011, Nature, 473, 349
Tinney, C. G., Burgasser, A. J., & Kirkpatrick, J. D. 2003, AJ, 126, 975
Torres, C. A. O., Quast, G. R., Melo, C. H. F., & Sterzik, M. F. 2008, in Young Nearby Loose Associations, ed. B. Reipurth, 757
Veras, D., & Raymond, S. N. 2012, MNRAS, 421, L117
Wahhaj, Z., Liu, M. C., Biller, B. A., et al. 2011, ApJ, 729, 139
Warren, S. J., Mortlock, D. J., Leggett, S. K., et al. 2007, MNRAS, 381, 1400
Wright, E. L., Eisenhardt, P. R. M., Mainzer, A. K., et al. 2010, AJ, 140, 1868
Yee, H. K. C., Gladders, M. D., Gilbank, D. G., et al. 2007 [arXiv:astro-ph/0701839]
Zapatero Osorio, M. R., Béjar, V. J. S., Martín, E. L., et al. 2002, ApJ, 578, 536
Zuckerman, B., Song, I., & Bessell, M. S. 2004, ApJ, 613, L65